Paleoceanography of the eastern Indian Ocean from ODP Leg 121 drilling on Broken Ridge

DAVID K. REA *Department of Geological Sciences, University of Michigan, Ann Arbor, Michigan 48109-1063*
JONATHAN DEHN *Institut Fuer Mineralogie, Ruhr-Universitaet Bochum, Bochum, Germany*
NEAL W. DRISCOLL *Lamont-Doherty Geological Observatory, Palisades, New York 10964*
JOHN W. FARRELL *Department of Geological Sciences, Brown University, Providence, Rhode Island 02912*
THOMAS R. JANECEK *Ocean Drilling Program, Texas A&M University, College Station, Texas 77840*
ROBERT M. OWEN *Department of Geological Sciences, University of Michigan, Ann Arbor, Michigan 48109-1063*
JAMES J. POSPICHAL *Department of Geology, Florida State University, Tallahassee, Florida 32306*
PURTYASTI RESIWATI *Department of Geology, University of Nebraska, Lincoln, Nebraska 68588*
ODP LEG 121 SCIENTIFIC PARTY*

ABSTRACT

Broken Ridge, in the eastern Indian Ocean, is overlain by about 1,600 m of middle Cretaceous to Pleistocene tuffaceous and carbonate sediments that record the oceanographic history of southern hemisphere mid- to high-latitude regions. Prior to about 42 Ma, Broken Ridge formed the northern part of the broad Kerguelen–Broken Ridge Plateau. During the middle Eocene, this feature was split by the newly forming Southeast Indian Ocean Ridge; since then, Broken Ridge has drifted north from about 55° to 31°S.

The lower part of the sedimentary section is characterized by Turonian to Santonian tuffs that contain abundant glauconite and some carbonate. The tuffs record a large but apparently local volcanic input that characterized the central part of Broken Ridge into the early Tertiary. Maestrichtian shallow-water (several hundred to 1,000 m depth) limestones and cherts accumulated at some of the highest rates ever documented from the open ocean, 4 to 5 g $(cm^2 \cdot 10^3\ yr)^{-1}$. A complete (with all biostratigraphic zones) Cretaceous-Tertiary boundary section was recovered from site 752. The first 1.5 m.y. of the Tertiary is characterized by an order-of-magnitude reduction in the flux of biogenic sediments, indicating a period of sharply reduced biological productivity at 55°S, following which the carbonate and silica sedimentation rates almost reach the previous high values of the latest Cretaceous. We recovered a complete section through the Paleocene that contains all major fossil groups and is more than 300 m thick, perhaps the best pelagic Paleocene section encountered in ocean drilling. About 42 Ma, Broken Ridge was uplifted 2,500 m in response to the intra-plateau rifting event; subsequent erosion and deposition has resulted in a prominent Eocene angular unconformity atop the ridge. An Oligocene disconformity characterized by a widespread pebble layer probably represents the 30 Ma sea-level fall. The Neogene pelagic ooze on Broken Ridge has been winnowed, and thus its grain size provides a direct physical record of the energy of the southern hemisphere drift current in the Indian Ocean for the past 30 m.y.

INTRODUCTION

Broken Ridge is an elongated plateau-like feature that rises 3,500 m above the surrounding sea floor in the southeastern Indian Ocean (Figs. 1 and 2). More than 1,500 m of post-middle Cretaceous, fairly shallow water (less than 1,500 m) sediments has accumulated on Broken Ridge, and these sediments record both the geologic history of this feature and the oceanographic history of the mid-latitude Indian Ocean. Herein, we examine this sedimentary record and present the major events in the evolution of Broken Ridge and the southeastern Indian Ocean.

Tectonic History

Broken Ridge originated as the northern flank of the broad Kerguelen–Broken Ridge Plateau and was detached from the main part of that feature during the Eocene. Various indications, including the dating of dredged basalts (R. Schlich, 1988, personal commun.) and the results of Legs 119 and 120 (Leg 119 Scientific Drilling Party, 1988; Leg 120 Scientific Drilling Party, 1988), suggest that the main constructional phase of the Kerguelen–Broken Ridge Plateau occurred during the Albian. The middle Cretaceous is an important time for constructional volcanism through most of the world's ocean basins; other important rises, Ontong-Java, Manihiki, and Hess, are of similar basement age (Rea and Vallier, 1983). Greater

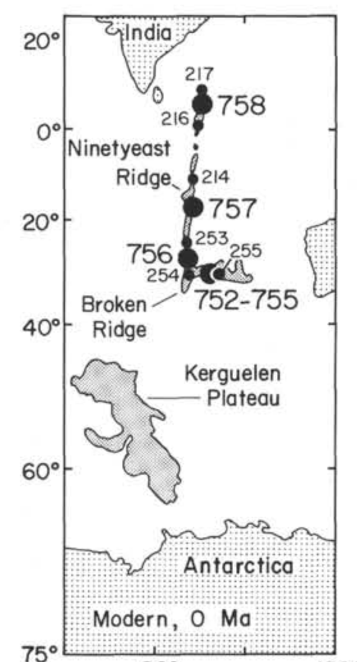

Figure 1. Map of the eastern Indian Ocean, showing the operational area of Leg 121 and DSDP and ODP drill sites.

*John Peirce and Jeffrey Weissel, Co-chief Scientists, and Elisabeth Fourtanier, Fred Frey, Paul D. Gamson, Jeffrey S. Gee, Ian L. Gibson, Chris Klootwijk, James R. Lawrence, Ralf Littke, Jerry S. Newman, Ritsuo Nomura, Andrew D. Saunders, Jan Smit, Guy M. Smith, Kensaku Tamaki, Elliott Taylor, Dominique Weis, and Craig Wilkinson.

Geological Society of America Bulletin, v. 102, p. 679–690, 12 figs., 3 tables, May 1990.

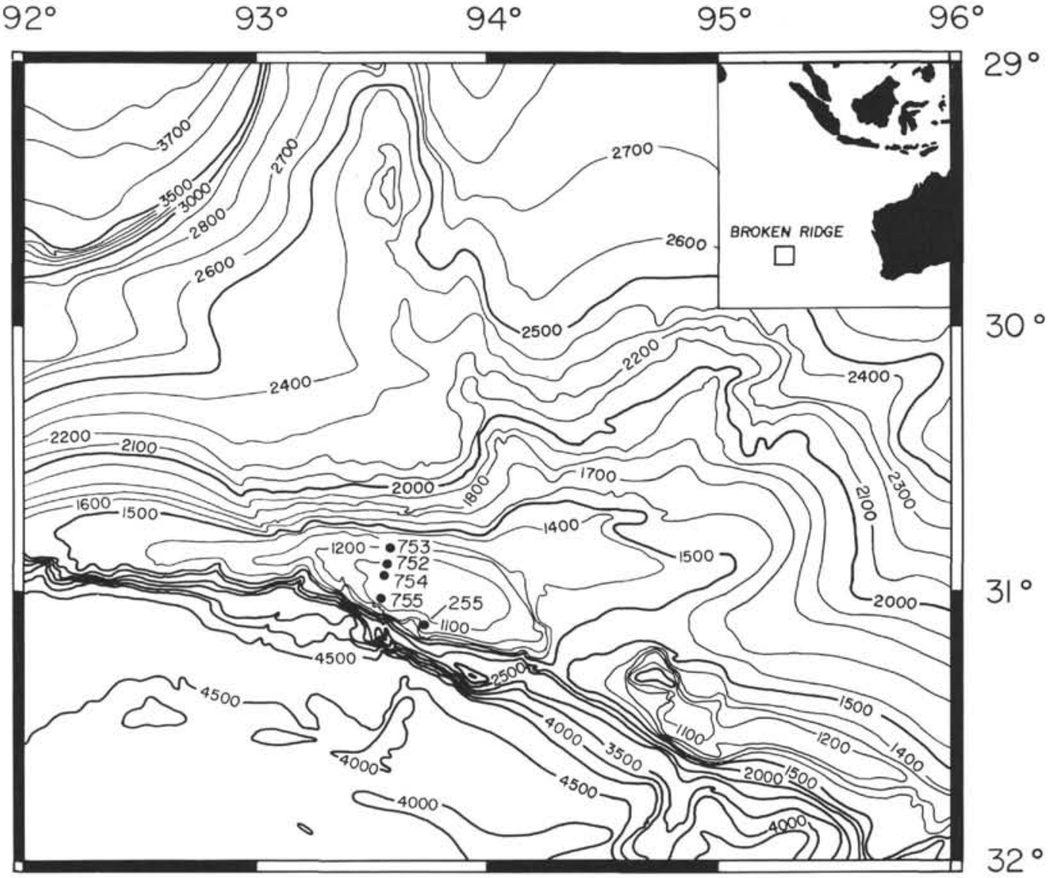

Figure 2. Bathymetric map of Broken Ridge, showing the locations of Leg 26 and Leg 121 drill sites. Depths are in meters.

Kerguelen apparently formed at or near the ridge crest in the then restricted seaway between Antarctica, recently separated India, and Australia.

About 60 m.y. after it was formed, Broken Ridge was uplifted by flexure that occurred in response to intra-plateau rifting. Following the rifting, sea-floor spreading began between the two parts of the old plateau at the Southeast Indian Ocean Ridge at anomaly 18 time, about 42 Ma (Houtz and others, 1977; Mutter and Cande, 1983). An important result of the Leg 121 drilling on Broken Ridge was to demonstrate that the Eocene rifting was not a thermal event, as there was no pre-rift arching or shoaling as would be expected in such circumstances. Furthermore, present heat-flow values are low, implying little additional heating associated with the rifting (Weissel and others, 1988). The rifting and uplift event is now seen as the pronounced angular unconformity that crosses the ridge crest (Fig. 3). Since the time of rifting, Broken Ridge has drifted north from its original position at about 55°S to its present location at 31°S.

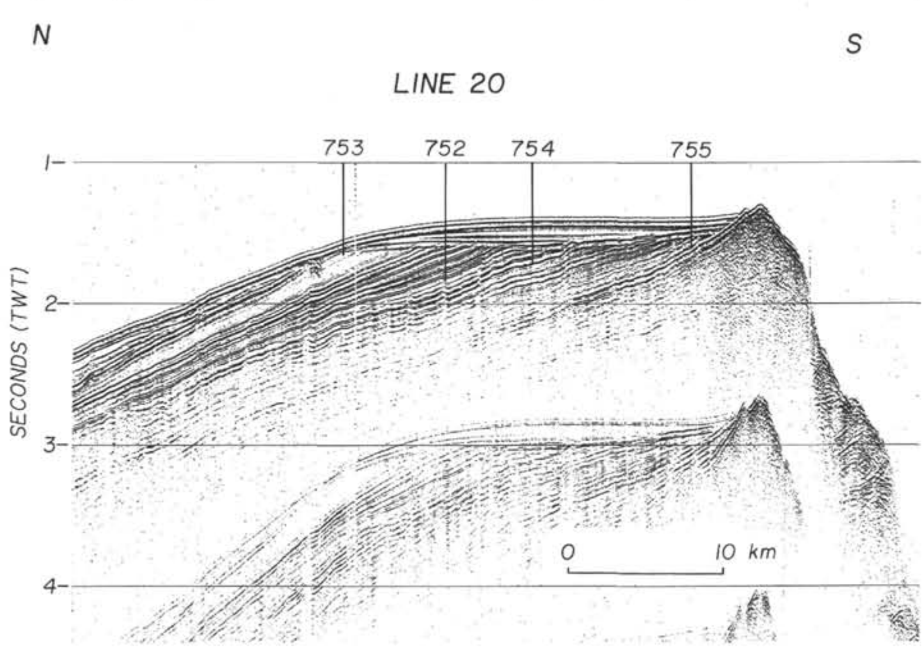

Figure 3. Seismic reflection profile across the crest of Broken Ridge in the vicinity of the Leg 121 drill sites. North is to the left.

Stratigraphy and Sediment Accumulation Rates

The biostratigraphy utilized in this report is based on the nannofossil stratigraphy as determined on board ship and as slightly revised at the Leg 121 post-cruise meeting in January of 1989 (Pierce, Weissel, and others, 1989). For Cenozoic materials, we use the zonations of Okada and Bukry (1980) as tied to the time scale of Berggren and others (1985). Mesozoic stratigraphy is based on the zonation of Sissingh (1977) as tied to the magnetic reversal time scale of Harland and others (1982) using the revisions proposed by Kent and Gradstein (1985).

Combining the shipboard biostratigraphic, lithologic, and physical-properties data permits

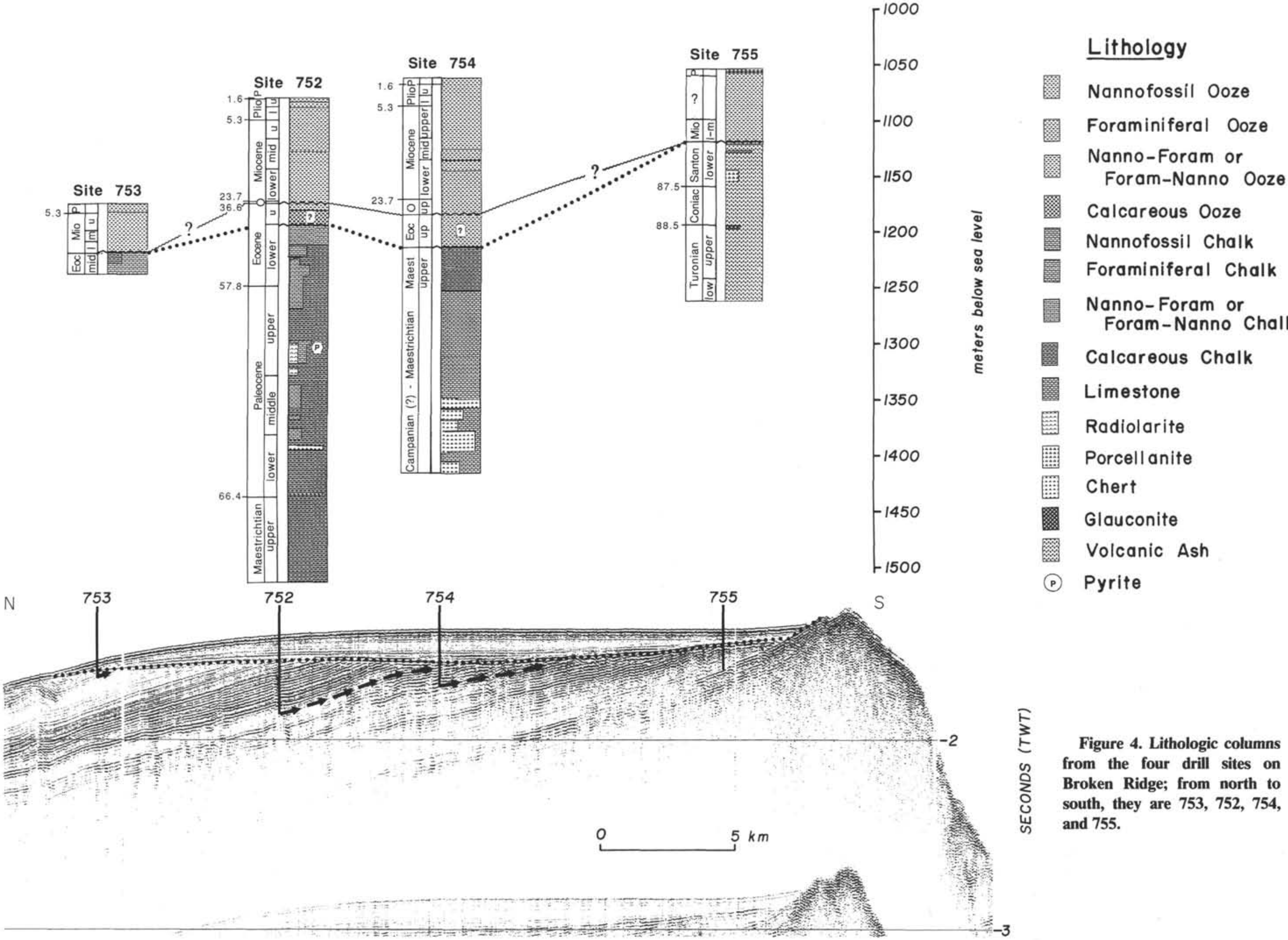

Figure 4. Lithologic columns from the four drill sites on Broken Ridge; from north to south, they are 753, 752, 754, and 755.

REPRINT

the calculation of rates of sediment deposition. The traditional value for deposition rate is the linear sedimentation rate (LSR), commonly measured in meters per million years ($m/10^6$ yr) or centimeters per thousand years ($cm/10^3$ yr). A more useful value to describe sediment deposition is the mass accumulation rate (MAR). MAR is a quantification of the true mass flux of sedimentary material to the sea floor and is the product of LSR and the dry bulk density (DBD):

$$\mathrm{MAR}\ [\mathrm{g}\ (\mathrm{cm}^2 \cdot 10^3\ \mathrm{yr})^{-1}] = \mathrm{LSR}\ (\mathrm{cm}/10^3\ \mathrm{yr}) \times \mathrm{DBD}\ (\mathrm{g}/\mathrm{cm}^3).$$

This value inherently accounts for the variable amounts of pore space in sediments, thus for compaction. When the total MAR values are multiplied by the weight percent of any sedimentary component, the flux of that component is also quantified, and so the pitfalls of interpreting relative-abundance data can be avoided.

LSR values are based on the nannofossil biostratigraphy; bulk density measurements were determined in the sediment laboratory of the *Resolution.* Because of the limitations of the sedimentation rate data, which are determinable for every zone, interpretations of the resulting data are useful for deciphering phenomena that occur on longer, tectonic time scales. We estimate the accuracy of these data to be ±20%; minor changes may not be significant.

Paleoceanographic Setting and Objectives

The elucidation of the paleoceanographic and paleoclimatic history of the southeastern Indian Ocean was one of the major objectives of the Leg 121 drilling. Broken Ridge has always been above the calcium carbonate compensation depth, thus permitting deposition of a fossiliferous calcareous sedimentary section. The angular unconformity (Fig. 3) associated with the Eocene rifting separates underlying, northerly dipping Cretaceous and lower Paleogene tuffs, limestones, and chalks from the overlying upper Paleogene and Neogene calcareous oozes.

TABLE 1. DSDP AND ODP DRILL SITES ON BROKEN RIDGE

Site	S. lat.	E. long.	Water depth	Penetration	Oldest seds.
255	31.131°	93.729°	1,144 m	108.5 m	Santonian
752	30.891°	93.578°	1,086.3 m	435.6 m	U. Maestrichtian
753	30.839°	93.590°	1,176.1 m	62.8 m	M. Eocene
754	30.941°	93.567°	1,063.6 m	354.7 m	L. Maestrichtian
755	31.030°	93.548°	1,057.9 m	208.4 m	Turonian

Four drill sites (752–755, Table 1) are located along a 21.2-km north-south profile extending across the shallow, about 1,100 m depth, platform of Broken Ridge (Figs. 2 and 3). The sedimentary record of these sites (Fig. 4) contains evidence for locally important volcanic activity, high Cretaceous and Paleocene biological productivity, events of the Cretaceous-Tertiary boundary at high southern latitudes, Eocene uplift and erosion, Oligocene sea-level changes, and Neogene current winnowing.

THE SEDIMENTARY SECTION ON BROKEN RIDGE

The Pelagic Cap

The shallow plateau region of Broken Ridge is immediately underlain by a nannofossil ooze with foraminifers. The ooze reaches a maximum thickness of about 120 m at site 754 and thins to the north and south (Figs. 3 and 4). A layer of sand with limestone and chert pebbles (Fig. 5) divides the ooze section into upper and lower parts. The upper ooze unit is Pleistocene to Oligocene in age, 0 to 30 m.y. old.

The lower part of the ooze sequence is darker brown and contains numerous large foraminifers; 1% or 2% sand-sized, iron-stained quartz grains; and abundant fossil material reworked from the underlying Paleogene and Cretaceous sediments. This interval of ooze is of latest Eocene age, roughly 38 to 40 m.y. old.

The pelagic cap of Broken Ridge apparently has been winnowed (Davies, Luyendyk, and others, 1974), perhaps by the southern hemisphere drift currents. To determine the extent of the winnowing, we conducted on-board grain size analyses of the bulk sediment of this unit at quasi-regular intervals from sites 752, 753, and 754. Grain size of purely pelagic sediment has been shown elsewhere to afford paleocurrent and sedimentary process information (van Andel, 1973; Ledbetter, 1979; Rea and Janecek, 1986). Results show large changes in the grain size of the bulk sediment, from 5.4ϕ (24μm) to 3.3ϕ (100 μm), which are systematic and coherent among the three drill sites studied (Fig. 6).

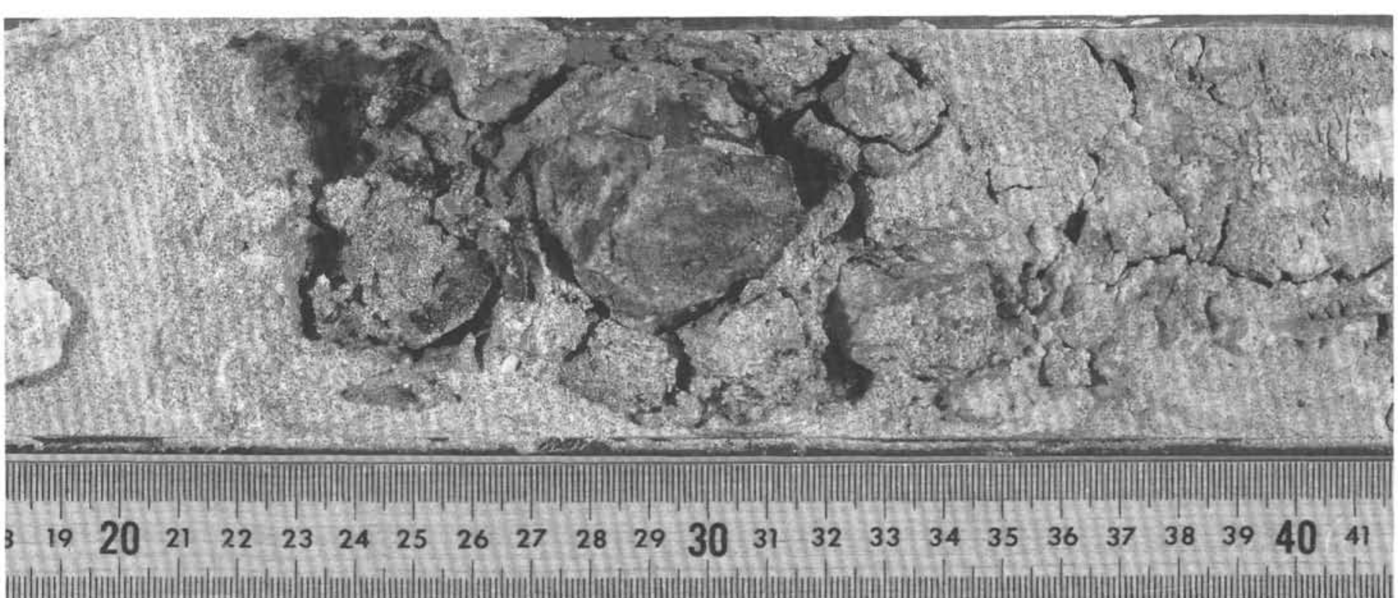

Figure 5. Limestone pebbles in ooze, recovered from the Oligocene disconformity at Hole 752A, core 10H, section 7.

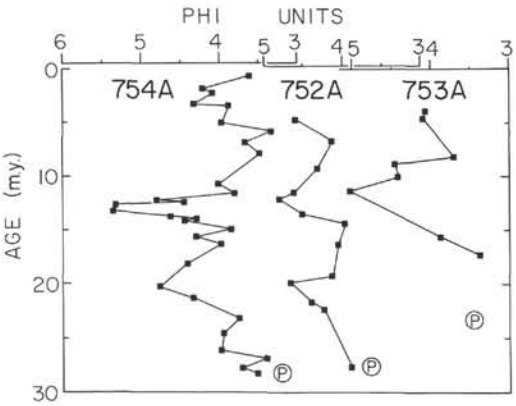

Figure 6. Bulk grain size of the Oligocene to Pleistocene pelagic ooze on Broken Ridge at Sites 754, 752, and 753. Data generated on board the *Resolution*, using the laser light-scattering technique of size analysis. Analyses were rapid and repeatable at sizes between about 9ϕ and 3.5ϕ. Larger particles, coarser than 80 to 100 μm, are probably under represented.

Poorly recovered nearshore deposits lie beneath the ooze unit on the upper Eocene erosion surface. This layer consists of quartz sand, dark chert and greenish-gray limestone pebbles, and shell hash mixed with Cretaceous through Eocene reworked carbonate material (Fig. 7). The Eocene and Oligocene pebble layers coalesce at either edge of the crest of Broken Ridge (Fig. 4). At the southern site, 755, the material lying on the Eocene-Oligocene erosion surface is a lower Miocene foraminifer sandstone, and the underlying Santonian limestones have been oxidized to a depth of 1.5 m (Fig. 8). Well logs suggest that this lower sand and gravel horizon may reach a thickness of 25 m at Site 754.

Lower Paleogene and Upper Cretaceous Carbonates and Cherts

Below the angular unconformity is nearly 1,200 m of sediment dominated by chalks and limestones and ranging in age from middle Eocene (45 m.y. old) at Site 753 to early Maestrichtian (75 m.y. old) at Site 754 (Fig. 4; Table 2). Opal and black chert are important components in the Paleocene chalks and Campanian limestones, respectively. The chalks are light colored to white in the upper part and darken to grayish green as ash content increases down section. Millimeter-scale green laminae that occur in bundles a centimeter or two thick are characteristic. These bundles in many cases exhibit scoured basal contacts, cross-laminae, and gradational coloration suggestive of graded bedding. Ash layers become common in the Maestrichtian carbonates. Microfaults, pyrite blebs, wavy laminae, and millimeter-sized dolomite rhombs, all indicative of increasing overburden and early diagenesis, occur in the lower part of carbonate series (Peirce, Weissel, and others, 1989).

The Cretaceous/Tertiary boundary occurs within the lower indurated chalk unit of Hole 752B at about 358 m below the sea floor. The boundary lies within a 60-cm-long ash-chert-chalk sequence (Fig. 9) that directly underlies a 5.5- to 6.5-m-thick ash layer. Details of the magnetic susceptibility data for this sequence suggest that the thick ash may be the result of multiple lesser ashfalls rather than one large one.

Santonian to Turonian Tuff

The lowest part of the Broken Ridge sedimentary section, recovered at Hole 755A, is 143 m of dark greenish-gray to black ash with limestone and glauconite of roughly late Santonian to early Turonian age, 83 to 90 m.y. Glauconite occurs throughout, in a more disseminated form in the upper parts of the hole, and in fining-upward units with sharp lower contacts in the lower few cores (Fig. 10). Numerous minor

Figure 7. Eocene sand and gravel recovered from the angular unconformity. Pebbles are of limestone, chert, and shell fragments; the size sorting probably results from drilling disturbance in this rotary-drilled core at Hole 754B, core 2R, section 1.

Figure 8. Miocene foraminiferal sandstone overlying oxidized (subaerially weathered?) Santonian limestone at Hole 755A, core 5R, section 1.

TABLE 2. MASS ACCUMULATION RATES OF SEDIMENT ON BROKEN RIDGE

Hole	Age (m.y.)	ΔT (m.y.)	Depth (mbsf)	ΔZ (m)	LSR	DBD	MAR
752A	0.0–1.9	1.9	0.0–4.3	4.3	0.23	0.86	0.20
	1.9–3.4	1.5	4.3–10.3	6.0	0.40	1.06	0.42
	3.4–5.0	1.6	10.3–19.1	8.8	0.55	1.02	0.56
	5.0–6.4	1.4	19.1–25.1	6.0	0.43	0.90	0.39
	6.4–14.3	7.9	25.1–58.1	33.0	0.42	0.96	0.40
	14.3–17.1	2.8	58.1–73.1	15.0	0.54	0.93	0.50
	17.1–23.7	6.6	73.1–91.7	18.6	0.28	1.10*	0.31
	23.7–28.2	4.5	91.7–93.4	1.7	0.04	1.01*	0.04
		unconformity					
	37.8		104.3				
		unconformity					
	55.3–57.8	2.5	115.6–171.3	55.7	2.23	1.37	3.06
	57.8–59.2	1.4	171.3–202.8	31.5	2.25	1.31	2.95
	59.2–60.0	0.8	202.8–219.7	16.9	2.11	1.45	3.06
	60.0–61.6	1.6	219.7–251.4	31.7	1.98	1.17	2.32
	61.6–62.0	0.4	251.4–297.7	46.2	11.55	1.32	15.25
752B	63.8–64.8	1.0	318.7–345.1	26.4	2.64	1.96	5.17
	64.8–65.9	1.1	345.1–353.9	8.8	0.80	2.05	1.64
	65.9–66.4	0.5	353.9–358.5	4.6	0.92	1.55	1.43
	66.4–69.0	2.6	358.5–422.3	63.8	2.45	1.98	4.86
			TD 435.6				
753A	0.0–1.9	1.9	0.0–1.0	1.0	0.05	0.99	0.05
	1.9–4.5	2.6	1.0–9.5	8.5	0.33	0.99	0.33
	4.5–8.2	3.7	9.5–17.0	7.5	0.20	0.94	0.19
	8.2–10.0	1.8	17.0–24.4	7.4	0.41	1.02	0.42
	10.0–16.2	6.2	24.4–34.4	10.0	0.16	1.08	0.17
	16.2–23.6	7.4	34.4–43.6	9.2	0.12	0.83	0.10
		unconformity					
	47.0–48.8	1.8	43.6–62.8	19.2†	1.07†	1.08	1.16†
			TD 62.8				
754A	0.0–1.9	1.9	0.0–6.3	6.3	0.33	0.89	0.30
	1.9–2.2	0.3	6.3–7.3	1.0	0.33	0.91§	0.30
	2.2–2.6	0.4	7.3–10.4	3.1	0.78	0.93	0.73
	2.6–3.5	0.9	10.4–16.0	5.6	0.62	1.05	0.65
	3.5–3.8	0.3	16.0–18.4	2.4	0.80	1.00	0.80
	3.8–5.0	1.2	18.4–24.0	5.6	0.47	0.98	0.46
	5.0–6.5	1.5	24.0–33.4	9.4	0.63	1.00	0.63
	6.5–12.0	5.5	33.4–47.5	14.1	0.26	0.96	0.25
	12.0–14.4	2.4	47.5–75.2	27.7	1.15	1.07	1.23
	14.4–15.4	1.1	75.2–81.6	6.4	0.58	0.97	0.56
	15.4–17.1	1.7	81.6–88.2	6.6	0.39	0.90	0.35
	17.1–21.5	4.4	88.2–91.3	3.1	0.07	0.86	0.06
	21.5–23.7	2.2	91.3–107.8	16.5	0.75	1.00	0.75
	23.7–28.2	4.5	107.8–115.3	7.5	0.17	0.97	0.17
	28.2–30.2	2.0	115.3–122.2	6.9	0.34	1.19	0.40
		unconformity					
754B	74.0 75.0	1.0	224.0–262.8	38.8	3.88	1.97	7.64
			TD 354.7				
755A**	0.0–1.9	1.9	0.0–7.1	7.1	0.37	0.96	0.36
	1.9–10.0	8.1	7.1–45.8	38.7	0.48	1.00††	0.48
	10.0–10.8	0.8	45.8–55.5	9.7	1.21	1.00††	1.21
	10.8–14.9	4.1	55.5–65.6	10.1	0.25	1.00††	0.2
		unconformity					
	83.0–86.6	3.6	65.6–91.5	25.9	0.72	1.98	1.43
	86.6–88.5	1.9	91.5–120.5	29.0	1.53	1.78	2.72
	88.5–89.5	1.0	120.5–169.7	49.2	4.92	1.96	9.64
			TD 208.4				

Note: LSR, linear sedimentation rate ($cm/10^3$ yr); DBD, dry bulk density (g/cm^3); MAR, mass accumulation rate or flux [$g(cm^2 \cdot 10^3\ yr)^{-1}$].
*Values from equation in Rea and others (1986).
†Minimum value only.
§Average of values above and below.
**Rotary coring; poor Neogene recovery.
††No data; estimated value.

components occur: porcellanite, shell fragments, pyrite, in some cases associated with the calcite veinlets, apatite and rare gypsum crystals found in vugs. The entire section displays mottles and burrow structures.

COMPARISON WITH THE SECTION RECOVERED FROM KERGUELEN PLATEAU

The composite section recovered from the central and northern parts of Kerguelen Plateau (Leg 119 Scientific Drilling Party, 1988; Leg 120 Scientific Drilling Party, 1988), those locations that might reasonably be expected to represent the same general sedimentary environment as do the Broken Ridge drill sites, is similar to the Broken Ridge composite section. Regional geologic units on Kerguelen Plateau include

1. Quaternary to upper Miocene diatom ooze that includes small percentages of foraminifers and nannofossils. Ice-rafted debris occurs in sediments younger than middle Pliocene.
2. Middle Miocene to Paleocene nannofossil ooze, in many cases with foraminifers. This unit is stark white in the younger parts but takes on more color, generally light greenish gray, with depth. Faint greenish laminae occur, as do minor intervals of chalk, chert, and porcellanite. A middle Eocene hiatus occurs within this unit.
3. Maestrichtian to Campanian chalk with black chert and green laminae. Glauconite (5% to 58% of the sediment) and glauconite sandstones occur lower in this unit. Indications of shallow-water deposition occur, including a 40-m-thick Maestrichtian series of gravels and breccias derived from volcanic basement that interrupts the pelagic limestones.
4. Santonian through Turonian pelagic limestone and chalk with clayey interlayers, shelly layers, layers with sharp lower contacts, and abundant glauconite.
5. Basalt. Silica-saturated transitional tholeiites (T-MORB) underlie lower Turonian and perhaps Cenomanian(?) limestones.

This composite section with its upper oozes, chalks with green laminae and black chert, and glauconitic limestones is similar to the Broken Ridge section. Three significant differences occur. The first is the vast quantities of ash recovered in the Broken Ridge sections, roughly two orders of magnitude more ash than occurs in the Kerguelen sections. This aspect of the Leg 121 recovery requires a large, local source of basaltic debris. Second, there is a greater extent of lithification or early diagenesis at the Broken Ridge sites than in the Kerguelen sediments, apparently the result of greater overburden in the more northerly locations. Finally, the Neogene sequence on Kerguelen records the great increase in silica productivity that occurred in the Antarctic Circumpolar Ocean during the late Cenozoic, a paleoceanographic event that occurred well to the south of the late Neogene paleoposition of Broken Ridge.

RATES OF SEDIMENT ACCUMULATION

The nannofossil ooze that forms the pelagic cap of Broken Ridge accumulated at 0.35 to 0.5 g ($cm^2 \cdot 10^3$ yr)$^{-1}$ (Table 2), values normal for oligotrophic mid-gyre shallow-water carbonate fluxes (Rea and Thiede, 1981; Thiede and Rea, 1981; Rea and Leinen, 1986a). The youngest chalks recovered below the angular unconformity at Site 753, of middle Eocene age, accumulated at rates of about 1.2 g ($cm^2 \cdot 10^3$ yr)$^{-1}$, rates slightly higher than normal for a low-

Figure 9. The lithologic section in Hole 752B, core 11R, section 3, 40–100 cm, from about 358 m below the sea floor, that contains the transition from Cretaceous to Tertiary fossils.

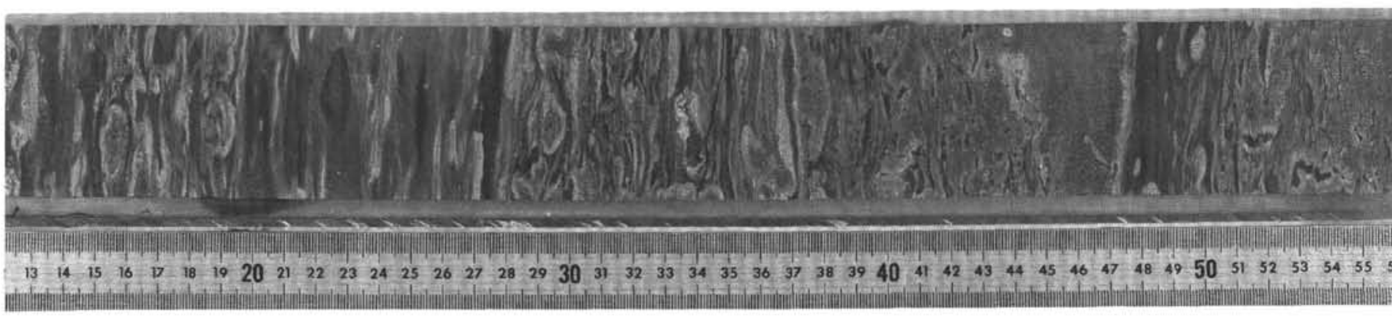

Figure 10. Bioturbated mixture of glauconite and ash and a glauconite turbidite in the Turonian tuffs of core 18R, section 1, of Hole 755A. Base of glauconite turbidite at 47 cm; soft-sediment deformation may occur at 14–19 and 28–45 cm.

productivity carbonate depositional environment. Rates increase down section. Lower Paleogene and upper Maestrichtian chalks have MAR values that average about 3.4 g ($cm^2 \cdot 10^3$ $yr)^{-1}$ through this interval with relatively low rates of 1.4 to 1.6 g ($cm^2 \cdot 10^3$ $yr)^{-1}$ at and just above the Cretaceous-Tertiary boundary and a higher rate of 4.9 g ($cm^2 \cdot 10^3$ $yr)^{-1}$ in the zone just below it (Table 2).

Biostratigraphic zonations are less detailed in the Maestrichtian chalk-limestone-chert sequence. Those data indicate a MAR of 7.6 g ($cm^2 \cdot 10^3$ $yr)^{-1}$. The underlying Santonian to Turonian ash, glauconite, and limestone unit has MAR's of 1.4 to 9.6 g ($cm^2 \cdot 10^3$ $yr)^{-1}$ (Table 2); these values are not so well constrained as those for the Maestrichtian limestones above.

The total flux of sediments can be proportioned among the various sedimentary components (Table 3; Fig. 11). The flux of calcium carbonate increases downcore from 0.4 g ($cm^2 \cdot 10^3$ $yr)^{-1}$ in the pelagic cap to 1.0 g ($cm^2 \cdot 10^3$ $yr)^{-1}$ in the middle Eocene chalks, 2.9 g ($cm^2 \cdot 10^3$ $yr)^{-1}$ in the Paleocene to upper Maestrichtian chalks, and 4.7 g ($cm^2 \cdot 10^3$ $yr)^{-1}$ in the Maestrichtian limestones. The lowermost unit dominated by the Santonian to Turonian ash has a $CaCO_3$ flux of 0.7 g ($cm^2 \cdot 10^3$ $yr)^{-1}$.

The ash flux also increases downcore (Table 3; Fig. 11). Ash entered the pelagic sediments of the upper unit in trace amounts only. Ash MAR in the middle Eocene chalks of Site 753 is 0.1 g ($cm^2 \cdot 10^3$ $yr)^{-1}$; in the Paleocene to upper Maestrichtian section, the ash flux is 0.6 g ($cm^2 \cdot 10^3$ $yr)^{-1}$; in the lower Maestrichtian limestones, the ash flux is 2.5 g ($cm^2 \cdot 10^3$ $yr)^{-1}$; and in the lowest, ash-rich rocks, the flux of volcanic material is 1.1 to 6.5 g ($cm^2 \cdot 10^3$ $yr)^{-1}$. These accumulation rate values for volcanic ash are among the largest ever recorded from within (not immediately overlying basement) oceanic sedimentary sections (Rea and Thiede, 1981) and denote important volcanic activity on the northeastern part of the Kerguelen–Broken Ridge Plateau.

Opal is an important sedimentary component in the Paleocene section, where siliceous materials accumulated at rates of 0.2 to 1.0 g ($cm^2 \cdot 10^3$ $yr)^{-1}$ (Table 3). Glauconite is an important component of the Santonian to Turonian ash-dominated unit and accumulated at about 1.9 g ($cm^2 \cdot 10^3$ $yr)^{-1}$ (Table 3).

THE PALEOCEANOGRAPHIC RECORD OF BROKEN RIDGE

Turonian to Santonian Volcanism

The ash-rich sediments of the Late Cretaceous indicate a somewhat unusual depositional environment on Broken Ridge. The volcanic component that dominates these sediments requires a large and local source of basaltic material. None of the surrounding drill sites, specifically Site 255 (20.7 km east-southeast of Site 755) but with very poor recovery; Sites 256, 257, and 258 (1,000 to 1,800 km to the north and east) (Davies, Luyendyk, and others, 1974); or any of the Leg 119-120 sites on Kerguelen, exhibit more than the normal trace amounts of Cretaceous ash. Very high fluxes of volcanogenic material combined with a truly local distribution of the deposit suggest that the Broken Ridge transect was within several tens of kilometers of the volcanic source. The ash was erupted subaerially, and so, if one assumes that the plateau lay beneath prevailing westerlies during the Cretaceous, the volcano lay to the west. Because information concerning the older geologic record is not available, it is not clear whether the volcanism is part of the waning phase, perhaps recently subaerial, of plateau construction or a distinctly separate and younger event.

Glauconite is an important component of these sediments and was incorporated into the ashy material at rates of as much as 1.9 g ($cm^2 \cdot 10^3$ $yr)^{-1}$. This component has a wide regional distribution, occurring in all the Kerguelen cores of equivalent age (Bitschene and others, 1989) and at Site 258 on the Naturaliste Plateau 1,800 km to the east (Davies, Luyendyk, and others, 1974). The normal environment of formation of glauconite is a shallow-water, outer-shelf, low- to very low-sedimentation-rate locale. Overlying waters are oxidizing, but the sediments themselves may be reducing; micro-reducing environments, such as within fecal pellets, may be

TABLE 3. PALEOGENE AND CRETACEOUS FLUXES OF MAJOR SEDIMENTARY COMPONENTS

Hole	Age (m.y.)	Total MAR	Percent abundance			Mass accumulation rate		
			$CaCO_3$	Opal	Ash	$CaCO_3$	Opal	Ash
753A	47.0–48.8	1.61	88	2	10	1.03	0.02	0.10
752A	55.3–57.8	3.06	81	6	13	2.48	0.18	0.40
	57.8–59.2	2.95	73	9	18	2.15	0.26	0.53
	59.2–60.0	3.06	82	9	9	2.51	0.28	0.28
	60.0–61.6	2.32	68	16	16	1.58	0.37	0.37
	61.6–62.1*	15.25*	73	13	14	11.13*	1.98*	2.14*
752B	63.8–64.8	5.17	62	19	19	3.21	0.98	0.98
	64.8–65.9	1.64	58	21	21	0.95	0.34	0.34
	65.9–66.4	1.43	30	5	65	0.43	0.07	0.93
	66.4–69.0	4.86	81	4	15	3.94	0.19	0.73
754B	74.0–75.0	7.64	61	6	33	4.66	0.46	2.52
				Glauc.			Glauc.	
755A	83.0–86.6	1.43	25	1	74	0.36	0.01	1.06
	86.6–88.5	2.72	18	2	80	0.49	0.05	2.18
	88.5–89.5	9.64	13	20	67	1.25	1.93	6.46

Note: mass accumulation rates in g$(cm^2 \cdot 10^3\ yr)^{-1}$.
*Short zone at core bottom is unreliable; averaged with above zone for plotting.

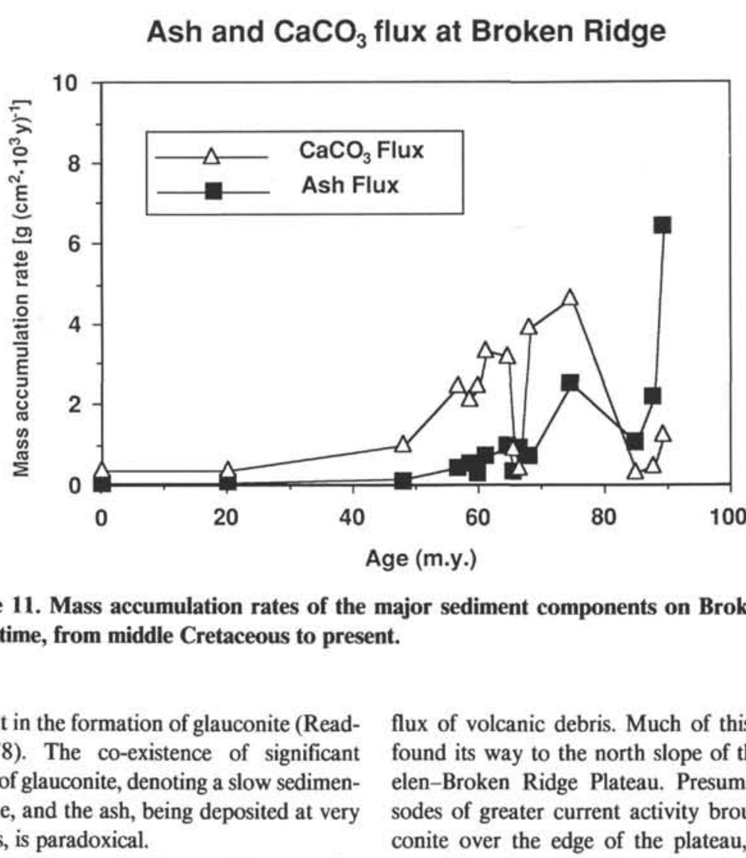

Figure 11. Mass accumulation rates of the major sediment components on Broken Ridge through time, from middle Cretaceous to present.

important in the formation of glauconite (Reading, 1978). The co-existence of significant amounts of glauconite, denoting a slow sedimentation rate, and the ash, being deposited at very high rates, is paradoxical.

One possible scenario that would account for these observations is as follows. The part of the sea floor that is now the crest of Broken Ridge must have been situated at the shelf-slope break on the northeastern margin of Kerguelen–Broken Ridge Plateau (Weissel and others, 1988). Glauconite formed in suitable locations all across the plateau in low-sedimentation-rate, low-productivity but carbonate-rich settings. This environment, recorded at several Kerguelen drill sites, was subjected to a large but local influx of volcanic debris. Much of this material found its way to the north slope of the Kerguelen–Broken Ridge Plateau. Presumably, episodes of greater current activity brought glauconite over the edge of the plateau, where it was disseminated with the hemipelagic ash and/or formed discrete downslope density flows, resulting in the glauconite turbidites of Site 755 (Fig. 10).

Maestrichtian Carbonate Platform

Volcanic ash continued as an important component of the Upper Cretaceous sediments. Fifteen million years after it was first recorded, ash fluxes were about 2.5 g $(cm^2 \cdot 10^3\ yr)^{-1}$ (Fig. 11), roughly half the average Turonian to Santonian flux. The source of this activity remained close at hand to the west; nearby drill sites do not contain any record of this ongoing Broken Ridge eruption.

Carbonate deposition increased markedly during this time span. Limestones and chalks accumulated at about 4.7 g $(cm^2 \cdot 10^3\ yr)^{-1}$ during the early Maestrichtian compared to 0.4 g $(cm^2 \cdot 10^3\ yr)^{-1}$ in the underlying ash-rich material (Table 3; Fig. 11). By comparison, carbonates on the Ontong-Java Plateau, Shatsky Rise, Manihiki Plateau, and the Magellan Rise accumulated through the later Cretaceous at rates of 1 to 2 g $(cm^2 \cdot 10^3\ yr)^{-1}$. Only Hess Rise, which was beneath the equatorial high-productivity zone at this time, has similar carbonate mass accumulation rates, 3.8 g $(cm^2 \cdot 10^3\ yr)^{-1}$ in the Campanian and Maestrichtian and 7.6 g $(cm^2 \cdot 10^3\ yr)^{-1}$ during the early Cenomanian and late Albian (Thiede and Rea, 1981; Vallier and others, 1983).

These high carbonate flux rates for the northeastern edge of Kerguelen–Broken Ridge Plateau require a setting of high biological productivity and most likely deposition above the paleolysocline. Chert, the alteration product of biogenic silica, is also an indicator of high biological productivity. The sediments are completely bioturbated, an indication of oxygenated, open-water environments.

The important question posed by these deposits concerns the nature of the source of nutrients necessary to sustain millions of years of apparently high biological productivity. Whatever the source, it became effective some time during the 8 m.y. unrepresented in the Leg 121 cores, between about 83 and 75 Ma. The time of 80 to 85 Ma is important around the world as a time of plate boundary rearrangement, changes in the rates and directions of plate motion, and the opening of oceanic gateways (Berggren and Hollister, 1977). Oceanic circulation between Antarctica and Australia may have started or become more pronounced at this time (Cande and Mutter, 1982; Mutter and others, 1985; Fig. 12). Furthermore, the northward motion of India, which became much more rapid than previously, also may have allowed true oceanic circulation in the proto–Indian Ocean south of the subcontinent (Fig. 12). Whatever the cause, some important change in oceanic circulation across Kerguelen–Broken Ridge Plateau is implicated in the large flux increase of biogenic sediments. Northward motion of the plateau was minimal during the Late Cretaceous, and so any new circulation patterns would have influenced regions at fairly high latitudes in the southern proto–Indian Ocean.

The great oceanic rises, when they project up into the realm of the ocean surface circulation, cause bathymetrically induced upwelling as those currents are forced upslope. This process occurs now over the Galapagos platform and happened during the Cretaceous over Hess Rise (Vallier and others, 1983). Nutrients are thereby brought into the photic zone, and productivity is enhanced. In the case of the Kerguelen–Broken Ridge Plateau, this scenario would further imply the development of a drift current in the southern proto-Indian Ocean about 80 to 85 m.y. ago since the plateau was already there. The increase in carbonate and silica productivity apparently records the evolution of the environment of Kerguelen–Broken Ridge Plateau from a restricted sea, shielded by India and Australia, to that of an open ocean, complete with drift currents.

Depositional Environments at the Cretaceous-Tertiary Boundary

The rock record of the Cretaceous-Tertiary boundary, recovered at Hole 752B, must be interpreted with some caution. The recovered materials occur as "drilling biscuits," 4- to 10-cm-long cylinders of rock that twist off during coring and are captured by the core barrel. There is no way of knowing how much material is missing between biscuits. The Cretaceous-Tertiary boundary occurs in section 3 of core 121-752B-11R (the ODP code is Leg–Hole–core–core type; R is for rotary drilled; Fig. 9). That section contains 10 biscuits, including chert biscuits in the middle of the 23-cm-long transition zone between sub-boundary Cretaceous foraminifera at 95 cm and supra-boundary Tertiary nannofossils at 72 cm. In general, most recovery loss is associated with cherts, and so there may be important components of the Cretaceous-Tertiary boundary section missing from core 121-752B-11R, section 3. The depositional environment is one of moderate energy, as indicated by horizontal laminations in the ash layers and soft-sediment deformation features; oxygenated bottom waters, as indicated by burrows and mottles; and continuing ash influx.

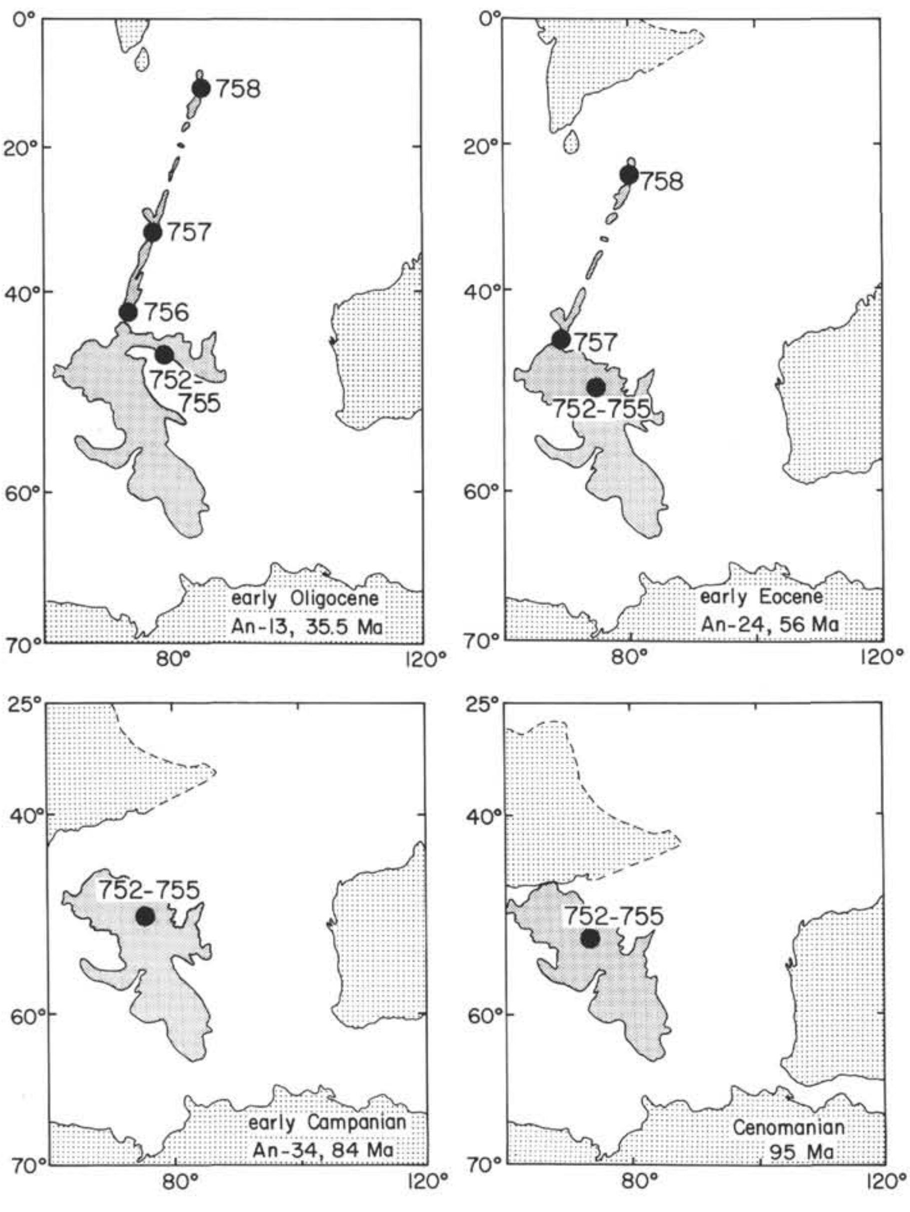

Figure 12. Backtrack-paleoposition diagrams of Ninetyeast Ridge, Broken Ridge, and Kerguelen Plateau. ODP Leg 121 drill sites shown as large dots. Reconstructions are taken from Royer and Sandwell (1989); note that subsidence is not accounted for in these figures.

Immediately overlying this boundary section is an ash layer that may exceed 6 m in thickness. Magnetic susceptibility data suggest that this thick unit is a compound ash layer, composed of several individual ash fall events. This unusual deposit may represent either a sudden, great influx of volcanic debris or a representation of the normal, ongoing ash flux in the absence of any carbonate input; the flux data permit differentiation between these possibilities (Table 3; Fig. 11). Volcanic ash MAR increases from 0.7 g $(cm^2 \cdot 10^3\ yr)^{-1}$ in the uppermost Maestrichtian zone to 0.9 g $(cm^2 \cdot 10^3\ yr)^{-1}$ in the lowest Paleocene zone, an increase barely larger than the estimated errors of calculation. At the same time, the mass accumulation rate of calcium carbonate falls by an order of magnitude, from 3.9 to 0.4 g $(cm^2 \cdot 10^3\ yr)^{-1}$ just above the boundary, almost an order-of-magnitude reduction of flux. Opal fluxes are also reduced across this boundary (Table 3). The important change in sedimentation at the Cretaceous-Tertiary boundary, then, is in the rate of deposition of the biogenic component; ash flux may increase only slightly.

The significant implication of this scenario is that the carbonate flux at Kerguelen–Broken Ridge Plateau was greatly reduced through the initial two zones of the Tertiary, a period of about 1.5 m.y. The nannofossils preserved in the thick ash unit constitute an assemblage of opportunistic "survivor species" that bloomed when previously dominant groups were no longer competitive or were absent (Pospichal and others, 1989; Peirce, Weissel, and others, 1989). The record is of an oceanic ecosystem lasting more than a million years where the combination of nutrient supply and the ambient carbonate-secreting organisms was suddenly insufficient to precipitate previously normal amounts of calcite (Smit, 1982; Hsü and McKenzie, 1985; Zachos and Arthur, 1986). Normal productivity resumed between 63.8 and 64.8 Ma (Table 3; Fig. 11).

Paleoenvironments of the Early Paleogene

The Paleocene and Eocene chalks record ongoing open-ocean, high-latitude deposition on the gradually subsiding northern margin of the Kerguelen–Broken Ridge Plateau. Sediment mass accumulation rates remain high. Biogenic components accumulated at rates of about 2.4 to 4.2 g $(cm^2 \cdot 10^3\ yr)^{-1}$; volcanic ash accumulated at rates as high as 1.0 g $(cm^2 \cdot 10^3\ yr)^{-1}$, still a large input value and one that records the waning eruptive cycle that began in the Mesozoic. Rates decline in the Eocene (Table 3; Fig. 11). Sediments of middle to late Paleocene age are enriched in diatoms and radiolarians. Biogenic silica exceeds 30% of the sediment, and opal fluxes were as much as 1.0 g $(cm^2 \cdot 10^3\ yr)^{-1}$ (Table 3), a high rate for open-ocean silica productivity; the flux of opal in the modern eastern equatorial Pacific is 0.1 to 0.2 g $(cm^2 \cdot 10^3\ yr)^{-1}$ (Lyle and others, 1988).

Information from foraminifers, both the benthic assemblages and the planktonic to benthic ratios, suggests that the lower Paleocene material accumulated in rather shallow water depths probably somewhere on the upper slope (Peirce, Weissel, and others, 1989). Paleodepths determined from these sorts of considerations gradually increase throughout the Paleocene and into the Eocene, reaching 1,000 to 1,500 m. The sedimentary structures in the lower and middle Paleogene materials, horizontal laminae with scoured lower contacts, cross-bedding, and graded bedding, are a direct indication of current velocities above the threshold of motion of silt, approximately 20 cm/s (Miller and others, 1977).

Sediments in the short middle Eocene section encountered at Site 753 exhibit ash MAR's of 0.1 g $(cm^2 \cdot 10^3\ yr)^{-1}$ or less, a more normal value for Eocene sediments; the long eruptive history of the nearby volcanic center was over. The flux of carbonates has dropped to about 1.0 g $(cm^2 \cdot 10^3\ yr)^{-1}$, low by Kerguelen–Broken Ridge standards, but normal for oceanic plateaus. The reduction in flux of biogenic material may connote ongoing subsidence, lowering the platform such that bathymetrically induced upwelling no longer occurred; reduced intensity of oceanic surface circulation; or migration of the sub-polar convergence away from the site.

Lacunae and Hiatauses

Two distinct limestone and chert pebble layers were encountered at Sites 255 (Davies, Luyendyk, and others, 1974), 752, and 754, each representing an important unconformity (Figs. 4, 5, 7, and 8). The older layer denotes the major angular unconformity atop Broken Ridge (Fig. 3) and, at Site 752, separates underlying lower Eocene chalk from overlying upper Eocene ooze. The age of the oldest material above this unconformity is about 38 m.y., and the youngest material below, recovered at Site 753, is about 45 m.y., and so the timing of this event that denotes the uplift of Broken Ridge at the time of rifting is well constrained and matches the estimated rifting age of 42 m.y. based on geophysics (Mutter and Cande, 1983). Calculations of basement subsidence, using the square root of age relationship and considering the effects of sediment loading (Davis and Lister, 1974; Detrick and others, 1977; Rea and Leinen, 1986b), added to the amount of material eroded from the ridge following uplift, indicate that the total uplift of Broken Ridge was about 2,500 m. This uplift must have happened in the course of, at most, 2 or 3 m.y., and possibly much more rapidly.

Exposed Cretaceous limestone and chert sequences were subjected to subaerial erosion (Fig. 8) and shed clastics down the north-facing dip slope, where they occur in the Eocene pebble and sand layer. Ensuing subsidence occasioned the resumption of open-water carbonate deposition, although in very shallow conditions as depicted by both the benthic foraminifera, some of which have suffered mechanical abrasion, and the large rounded quartz grains in the upper Eocene ooze (Peirce, Weissel, and others, 1989).

The younger pebble and sand layer (Fig. 5) marks a disconformity that separates upper Eocene ooze from upper Oligocene ooze. The oldest age of the overlying sediment is about 30 m.y., and the youngest age of the underlying material is about 38 m.y. Early to late Oligocene microfossils are mixed in with this pebble layer. The Oligocene hiatus on Broken Ridge could result from either a relative fall in sea level or an intensification of ocean circulation. Kennett (1977), noting the occurrence of lower Oligocene hiatuses, has suggested that ocean circulation in the southern hemisphere became more intense at the time of the ice volume increase at the Eocene/Oligocene boundary, presumably in response to heightened pole-to-equator temperature gradients.

The presence of the widespread pebble and sand layer with clasts as much as 5 to 6 cm in diameter (Fig. 5) implicates a change in relative sea level as the cause of this event, as the other alternative, an increase in oceanic current velocity, would neither expose the rocks of Broken Ridge to further erosion nor occasion the transport of large pebbles. Because details of the post-rifting subsidence history of Broken Ridge are not yet clear, there can be no well-constrained estimate of the magnitude of the mid-Oligocene sea-level fall at this mid-ocean location.

Neogene Paleocurrents

Above the Oligocene disconformity lies an apparently complete Neogene section of foraminiferal and nannofossil oozes. This section accumulated at average rates of 0.35 to 0.5 g $(cm^2 \cdot 10^3\ yr)^{-1}$ (Table 2; Fig. 11), a much lower rate than in the Paleogene section below. The combination of shallow depths, high percentage of foraminifers, and lower carbonate MAR are all consistent with the interpretation of the DSDP Leg 26 scientists that this unit is a winnowed foraminifer nannofossil silt and sand layer (Davies, Luyendyk, and others, 1974). If this interpretation is correct, then the bulk grain size of these sediments should provide an indication of current velocity across Broken Ridge.

Broken Ridge has subsided by about 1,100 m since the post-rifting resumption of sedimentation about 38 m.y. ago. If the only process affecting the winnowing energy across the crest of Broken Ridge were subsidence, then the grain size of those sediments would be expected to display a smooth, upward-fining sequence. Any additional character in the grain size curve represents additional processes. Two such processes are especially likely: changes in relative sea level and fluctuations in the velocity of ocean currents. Rises in relative sea level would result in a lower-energy sea floor and deposition of smaller grains, whereas a coarsening-upward sequence might reflect a fall in sea level. Similarly, stronger ocean currents would be expected to remove finer grains, leaving a lag deposit of coarser sediment. The downcore grain size determinations of sediments from Sites 752, 753, and 754 conducted on board the *Resolution* show fluctuations that are temporally coherent from site to site (Fig. 6).

The size of the winnowed grains decreased during the late Oligocene and earliest Miocene from 30 to 20 Ma, increased during the late early Miocene from 20 to about 16 Ma, decreased from 16 to 13 Ma, increased through the middle and late Miocene from 13 to about 6 Ma, decreased into the early Pliocene to a low at about 2.5 or 3 Ma, and may have increased during the Pleistocene (Fig. 6). Of these several transitions, the one most likely to be related to a change in relative sea level is the lowermost, the upward-fining sequence of the upper Oligocene and lowermost Miocene. This change, which begins with the middle Oligocene pebble layer, apparently reflects increasing water depths on Broken Ridge as subsidence continued relatively rapidly and eustatic sea level rose, following the 30 Ma lowstand, to a relative high at 21 Ma (Haq and others, 1987). Although we cannot completely discount the effects of ensuing lesser eustatic sea-level changes, the remaining changes in grain size are interpreted to reflect changes in the circulation intensity of the wind-driven geostrophic drift current on the southern side of the southern hemisphere subtropical gyre. There is no correlation between the grain size variations shown in Figure 6 and the occurrence of hiatuses in other deep-sea sections (Keller and Barron, 1987). Since 30 m.y. ago, the Broken Ridge platform has moved north through about 15° of latitude, starting from about 46°S.

The grain size data suggest that the intensity of ocean circulation increased three times during the Neogene, 20–16, 13–6, and since 2.5 Ma, and decreased 16–13 and 6–2.5 Ma (Fig. 6). Important paleoclimatic changes occurred in the Miocene, changes that are usually linked with episodes of ice volume growth on Antarctica. Paleoclimatologists have generally assumed that increased ice volume can be equated with colder polar temperatures, steeper pole-to-equator temperature gradients, and thus more vigorous atmospheric and oceanic circulation. The weak link in this presumptive chain is the intuitive coupling of ice volume and temperature at the poles; the other assumptions are better demonstrated from observation.

The events of 16 to 13 Ma are a particularly good example of this. This was the time of an important ice volume increase on Antarctica (Woodruff and others, 1981; Vincent and others, 1985; Miller and others, 1987; Prentice and Matthews, 1988), enough to cause a 1 permil enrichment of oceanic $\delta^{18}O$ values for benthic foraminifera. This event would also have caused a eustatic sea-level fall and, presumably, significantly intensified atmospheric and oceanic circulation. Both of these consequences would tend to result in coarser grain size of winnowed deposits; yet, this was most clearly a time of increasingly finer grains in all three Broken Ridge sections (Fig. 6). The middle to late Miocene is thought to be a time of steady or perhaps decreasing ice volume (Miller and others, 1987), and yet there was a constant coarsening of the winnowed grains from 12 to 6 Ma. These observations suggest that the circulation intensity of the ocean (Woodruff and Savin, 1989) is not directly linked to polar ice volume. Other information suggests that the intensity of southern hemisphere atmospheric circulation appears to have increased at this later time, between 11 and 9 Ma, rather than earlier during the ice volume increase (Rea and Bloomstine, 1986; Woodruff and Savin, 1989). The latest Miocene southern hemisphere ice buildup event at about 5 Ma (Hodell and Kennett, 1986) also corresponds to a time of decreasing grain size on Broken Ridge, and so the Miocene pattern is consistent.

The implications are that a moisture supply threshold (Ruddiman and McIntyre, 1984) may be more important for significant ice buildup, rather than any further reduction in the temperature of polar regions. Southern hemisphere temperature reductions may follow ice buildup by a few million years, as snow-covered and high-albedo regions slowly increase in altitude or in area. The northern and southern hemispheres may behave differently in this respect, as Antarctic high-albedo regions are effectively limited by the ocean, whereas the continents of the northern hemisphere permit the rapid expansion of snow-covered high-albedo regions.

The younger part of the grain size record, the early Pliocene minima, corresponds with the known last time of equitable climates before the onset of northern hemisphere glaciation at 2.4 or 2.5 Ma.

SUMMARY

Kerguelen–Broken Ridge Plateau was formed by constructional volcanism during middle Cretaceous, presumably Albian, time. This broad depositional platform has remained within 1 or 2 km of sea level throughout its history and has accumulated a predominantly biogenic sedimentary section of limestones, chalks, and cherts. At the very northern edge of this broad submarine bank, a strong but local volcanic center provided significant ash deposits for more than 30 m.y., from 90 to 60 Ma.

In Turonian through Santonian time, most of the Kerguelen–Broken Ridge Plateau was a shallow open-ocean carbonate bank, receiving a low to moderate flux of calcium carbonate, perhaps 0.7 g $(cm^2 \cdot 10^3\ yr)^{-1}$, and was the site of extensive glauconite formation. At approximately 80 to 85 m.y. ago, the biological productivity of the overlying waters was greatly increased; the flux of carbonate increased to about 4.7 g $(cm^2 \cdot 10^3\ yr)^{-1}$ (Fig. 11). These Late Cretaceous carbonate fluxes are among the highest ever recorded on oceanic plateaus and require an environment of ongoing high biological productivity. They denote a combination of increased oceanic circulation, perhaps the result of widening of the Australo-Antarctic and proto–Indian Oceans (Fig. 12), and of bathymetrically induced upwelling of the surface waters. The Broken Ridge volcanic center continued to be a source of important amounts of ash during the latest Cretaceous (Fig. 11).

The Cretaceous-Tertiary boundary was recovered in Hole 752B. These sediments consist of the typical chalk-chert-ash layer sequence that had preceded that time for 8 m.y. or so. The mass accumulation rate of calcium carbonate dropped by an order of magnitude at the boundary and remained low for the first 1.5 m.y. of the Tertiary, indicating a significant and continuing reduction in the overall rate of biological productivity. At the same time, the input of volcanic ash rose slightly (Fig. 11).

Carbonate and opal deposition rates recovered from the low values that pertained immediately following the Cretaceous-Tertiary boundary and continued high through the Paleocene, providing an expanded and fossiliferous high-latitude section. Carbonate accumulated at 2.1 to 3.2 g $(cm^2 \cdot 10^3\ yr)^{-1}$, and the volcanic input was reduced to 0.5 g $(cm^2 \cdot 10^3\ yr)^{-1}$, indicating the waning of the long period of volcanic activity on the northern part of Kerguelen–Broken Ridge Plateau. By middle Eocene time, these fluxes had been reduced to about 1.0 g $(cm^2 \cdot 10^3\ yr)^{-1}$ for carbonate and 0.1 g $(cm^2 \cdot 10^3\ yr)^{-1}$ for volcanic material, both normal values for oceanic shallow-water depositional settings. The Late Cretaceous through middle Eocene record is one of decreasing ash input, waning biological productivity from very high to normal values, and gentle subsidence (Fig. 11).

An episode of uplift and erosion occurred in the middle Eocene. The sedimentary units were tilted gently northward and eroded, producing the striking angular unconformity seen in the seismic profiles (Fig. 3). Clastics, mostly pebbles of limestone and chert mixed with sand from the uplifted sediments, were shed northward along the exposed surface of the ridge and reworked into sand and gravel layers as it subsided through sea level. The total amount of vertical uplift at the south edge of Broken Ridge was about 2,500 m.

The Oligocene to Pleistocene history of Broken Ridge is one of post-rifting subsidence and northward drift (Fig. 12) to its present location near 31°S. A middle Oligocene disconformity, denoted by a pebble and sand layer, occurs within the pelagic unit atop the ridge and probably records the 30 Ma fall in eustatic sea level.

Upper Oligocene through Pleistocene carbonate oozes were deposited on this shallow platform at oligotrophic flux rates, about 0.35 to 0.5 g $(cm^2 \cdot 10^3\ yr)^{-1}$, and have been subjected to winnowing during the past 30 m.y. The winnowing record suggests, among other things, reduced ocean circulation intensity during times of southern hemisphere ice volume increase in the

Miocene, an observation that contradicts the general assumption of significant polar cooling causing enhanced circulatory vigor at times of ice volume increase.

ACKNOWLEDGMENTS

The SEDCO and ODP crew on board the *JOIDES Resolution* (*SEDCO-BP 471*) are a professional and capable group. We are particularly indebted to Dave Huey and the ODP drilling engineers and to Burney Hamlin and the technician staff for making Leg 121 a well-run and successful cruise. Martin Lagoe and an anonymous reviewer provided comments on this manuscript, and we appreciate their several helpful suggestions. All authors were supported by the multinational Ocean Drilling Program; efforts of the first author are supported in part by National Science Foundation Grant OCE88-11299.

REFERENCES CITED

Berggren, W. A., and Hollister, C. D., 1977, Plate tectonics and paleocirculation—Commotion in the ocean: Tectonophysics, v. 38, p. 11–48.

Berggren, W. A., Kent, D. V., Flynn, J. J., and van Couvering, J. A., 1985, Cenozoic geochronology: Geological Society of America Bulletin, v. 96, p. 1407–1418.

Bitschene, P. R., Breza, J., Holmes, M. A., and leg 120 Shipboard Party, 1989, Composition and geotectonic significance of Cr-rich glauconitic sediments from Site 748 (Leg 120, Kerguelen Plateau, southern Indian Ocean) [abs.]: Washington, D.C., International Geological Congress, 28th, v. 1, p. 156–157.

Cande, S. C., and Mutter, J. C., 1982, A revised identification of the oldest sea-floor spreading anomalies between Australia and Antarctica: Earth and Planetary Science Letters, v. 58, p. 151–160.

Davies, T. A., Luyendyk, B. P., and others, 1974, Initial reports of the Deep Sea Drilling Project (Volume 26): Washington, D.C., U.S. Government Printing Office, 1,129 p.

Davis, E. E., and Lister, C.R.B., 1974, Fundamentals of ridge crest topography: Earth and Planetary Science Letters, v. 21, p. 405–413.

Detrick, R. S., Sclater, J. G., and Thiede, J., 1977, The subsidence of aseismic ridges: Earth and Planetary Science Letters, v. 34, p. 185–196.

Haq, B. U., Hardenbol, J., and Vail, P. R., 1987, Chronology of fluctuating sea levels since the Triassic: Science, v. 235, p. 1156–1167.

Harland, W. B., Cox, A. V., Llewellyn, P. G., Pickton, C.A.G., Smith, A. G., and Walters, R., 1982, A geologic time scale: Cambridge, United Kingdom, Cambridge University Press, 131 p.

Hodell, D. A., and Kennett, J. P., 1986, Late Miocene–early Pliocene stratigraphy and paleoceanography of the South Atlantic and southwest Pacific Oceans: A synthesis: Paleoceanography, v. 1, p. 285–311.

Houtz, R. E., Hayes, D. E., and Markl, R. G., 1977, Kerguelen Plateau bathymetry, sediment distribution and crustal structure: Marine Geology, v. 25, p. 95–130.

Hsü, K. J., and McKenzie, J. A., 1985, A "strangelove" ocean in the earliest Tertiary, *in* Sundquist, E. T., and Broecker, W. S., eds., The carbon cycle and atmospheric CO_2: Natural variations Archean to present: Washington, D.C., American Geophysical Union Geophysical Monograph 32, p. 487–492.

Keller, G., and Barron, J. A., 1987, Paleodepth distribution of Neogene deep-sea hiatuses: Paleoceanography, v. 2, p. 697–713.

Kennett, J. P., 1977, Cenozoic evolution of Antarctic glaciation, the circum-Antarctic Ocean, and their impact on global paleoceanography: Journal of Geophysical Research, v. 82, p. 3843–3859.

Kent, D. V., and Gradstein, F. M., 1985, A Cretaceous and Jurassic geochronology: Geological Society of America Bulletin, v. 96, p. 1419–1427.

Ledbetter, M. T., 1979, Fluctuations of Antarctic bottom water velocity in the Vema Channel during the last 160,000 years: Marine Geology, v. 33, p. 71–89.

Leg 119 Scientific Drilling Party, 1988, Leg 119 studies climatic history: Geotimes, v. 33(7), p. 14–16.

Leg 120 Scientific Drilling Party, 1988, Leg 120 explores origins and history: Geotimes, v. 33(9), p. 12–16.

Lyle, M., Murray, D. W., Finney, B. P., Dymond, J., Robbins, J. M., and Brooksforce, K., 1988, The record of late Pleistocene biogenic sedimentation in the eastern tropical Pacific Ocean: Paleoceanography, v. 3, p. 39–59.

Miller, K. G., Fairbanks, R. G., and Mountain, G. S., 1987, Tertiary oxygen isotope synthesis, sea level history, and continental margin erosion: Paleoceanography, v. 2, p. 1–19.

Miller, M. C., McCave, I. N., and Komar, P. D., 1977, Threshold of sediment motion under unidirectional currents: Sedimentology, v. 24, p. 507–527.

Mutter, J. C., and Cande, S. C., 1983, The early opening between Broken Ridge and Kerguelen Plateau: Earth and Planetary Science Letters, v. 65, p. 369–376.

Mutter, J. C., Hegarty, K. A., Cande, S. C., and Weissel, J. K., 1985, Breakup between Australia and Antarctica: A brief review in the light of new data: Tectonophysics, v. 114, p. 255–279.

Okada, H., and Bukry, D., 1980, Supplementary modification and introduction of code numbers to the low-latitude coccolith biostratigraphic zonation (Bukry, 1973, 1975): Marine Micropaleontology, v. 5, p. 321–325.

Peirce, J., Weissel, J. K., and others, 1989, Proceedings of the Ocean Drilling Program, initial reports (Volume 121): College Station, Texas, Ocean Drilling Program, (in press).

Pospichal, J. J., Resiwati, P., Smit, J., Gamson, P. D., Nomura, R., Fourtanier, E., Peirce, J., Weissel, J., and ODP Leg 121 Shipboard Party, 1989, Calcareous nannofossils across continuous Cretaceous-Tertiary boundary sequence, Leg 121, Site 752, eastern Indian Ocean [abs.]: Washington, D.C., International Geological Congress, 28th, v. 2, p. 629.

Prentice, M. L., and Matthews, R. K., 1988, Cenozoic ice-volume history: Development of a composite oxygen isotope record: Geology, v. 16, p. 963–966.

Rea, D. K., and Bloomstine, M. K., 1986, Neogene history of the South Pacific tradewinds: Evidence for hemispherical asymmetry of atmospheric circulation: Palaeogeography, Palaeoclimatology, Palaeoecology, v. 55, p. 55–64.

Rea, D. K., and Janecek, T. R., 1986, Grain size changes in reworked pelagic sediments, Deep Sea Drilling Project site 599, *in* Leinen, M., Rea, D. K., and others, Initial reports of the Deep Sea Drilling Project (Volume 92): Washington, D.C., U.S. Government Printing Office, p. 341–343.

Rea, D. K., and Leinen, M., 1986a, Neogene controls on hydrothermal activity and paleoceanography of the southeast Pacific Ocean, *in* Leinen, M., Rea, D. K., and others, Initial reports of the Deep Sea Drilling Project (Volume 92): Washington, D.C., U.S. Government Printing Office, p. 597–617.

——— 1986b, Crustal subsidence and calcite deposition in the South Pacific Ocean, *in* Leinen, M., Rea, D. K., and others, Initial reports of the Deep Sea Drilling Project (Volume 92): Washington, D.C., U.S. Government Printing Office, p. 299–303.

Rea, D. K., and Thiede, J., 1981, Mesozoic and Cenozoic mass accumulation rates of the major sediment components in the Nauru Basin, western equatorial Pacific, *in* Larson, R. L., Schlanger, S. O., and others, Initial reports of the Deep Sea Drilling Project (Volume 61): Washington, D.C., U.S. Government Printing Office, p. 549–555.

Rea, D. K., and Vallier, T. L., 1983, Two Cretaceous volcanic episodes in the western Pacific Ocean: Geological Society of America Bulletin, v. 94, p. 1430–1437.

Rea, D. K., Chambers, L. W., Chuey, J. M., Janecek, T. R., Leinen, M., and Pisias, N. G., 1986, A 420,000-year record of cyclicity in oceanic and atmospheric processes from the eastern equatorial Pacific: Paleoceanography, v. 1, p. 577–586.

Reading, H. G., ed., 1978, Sedimentary environments and facies: Oxford, United Kingdom, Blackwell Scientific, 569 p.

Royer, J.-Y., and Sandwell, D. T., 1989, Evolution of the eastern Indian Ocean since the Late Cretaceous: Constraints from Geosat altimetry: Journal of Geophysical Research, v. 94, p. 13755–13782.

Ruddiman, W. F., and McIntyre, A., 1984, An evaluation of ocean-climate theories on the North Atlantic, *in* Berger, A. J., Imbrie, J., Hays, J., Kukla, G., and Saltzman, B., eds., Milankovitch and climate, understanding the response to orbital forcing: Dordrecht, the Netherlands, D. Reidel, p. 671–686.

Sissingh, W., 1977, Biostratigraphy of Cretaceous calcareous nannoplankton: Geologie en Mijnbouw, v. 56, p. 37–56.

Smit, J., 1982, Extinction and evolution of planktonic foraminifera after a major impact at the Cretaceous/Tertiary boundary: Geological Society of America Special Paper 190, p. 329–352.

Thiede, J., and Rea, D. K., 1981, Mass accumulation rates of Barremian to Recent biogenic sediments from the Mid-Pacific Mountains (Deep Sea Drilling Project Site 463) and Hess Rise (Sites 464, 465, 466), central North Pacific Ocean, *in* Thiede, J., Vallier, T. L., and others, Initial reports of the Deep Sea Drilling Project (Volume 62): Washington, D.C., U.S. Government Printing Office, p. 637–651.

Vallier, T. L., Dean, W. E., Rea, D. K., and Thiede, J., 1983, Geologic evolution of Hess Rise, central North Pacific Ocean: Geological Society of America Bulletin, v. 94, p. 1289–1307.

van Andel, Tj. H., 1973, Texture and dispersal of sediments in the Panama Basin: Journal of Geology, v. 81, p. 434–457.

Vincent, E., Killingley, J. S., and Berger, W. H., 1985, Miocene oxygen and carbon isotope stratigraphy of the tropical Indian Ocean, *in* Kennett, J. P., ed., The Miocene ocean: Paleoceanography and biogeography: Geological Society of America Memoir 163, p. 103–130.

Weissel, J. K., and the ODP Leg 121 Scientific Party, 1988, Tectonic history of Broken Ridge from ODP Leg 121 drilling and marine geophysical data: EOS (American Geophysical Union Transactions), v. 69, p. 1431–1432.

Woodruff, F., and Savin, S. M., 1989, Miocene deepwater oceanography: Paleoceanography, v. 4, p. 87–140.

Woodruff, F., Savin, S. M., and Douglas, R. G., 1981, Miocene stable isotope record: A detailed deep Pacific Ocean study and its paleoclimatic implications: Science, v. 212, p. 665–668.

Zachos, J. C., and Arthur, M. A., 1986, Paleoceanography of the Cretaceous/Tertiary boundary event: Inferences from stable isotopic and other data: Paleoceanography, v. 1, p. 5–26.

Manuscript Received by the Society March 23, 1989
Revised Manuscript Received August 23, 1989
Manuscript Accepted September 8, 1989

Printed in U.S.A.